A semi-Lagrangian method of solving the vorticity advection equation

By J. S. SAWYER

(Manuscript received June 17, 1963)

ABSTRACT

The basic equation of the barotropic model atmosphere is solved by following the motion of a system of atmospheric parcels each of which conserves its vorticity. The wind field is computed at intervals from the vorticity field on a fixed grid and is used as a basis for calculating the motion of the parcels. Results have similar accuracy to those obtained by Eulerian methods, but being independent of the latter, serve to indicate some effects of truncation error in the usual Eulerian scheme. The semi-Lagrangian scheme is suitable for integrations with long time steps on a coarse grid.

1. Introduction

It is well known that finite-difference methods of solving the vorticity–advection equation, and other similar equations, introduce errors into numerical predictions of the atmospheric flow. There have been a number of theoretical studies of the nature and magnitude of such truncation errors (for example GATES, 1959) and studies of the errors produced when finite difference methods operate on artificial analytical initial data fields for which the solutions are known (GATES & RIEGEL, 1962; MYAKODA, 1962). However, the effect of truncation errors in calculations based on synoptic data is not fully known, and there is therefore some interest in alternative integration procedures which have very different error characteristics, and in comparisons of the results with those of the more usual integration procedures.

The usual integration technique employed in computations involved in the barotropic forecasting model employs the vorticity advection equation in Eulerian form

$$\frac{\partial \eta}{\partial t} + J(\psi, \eta) = 0 \qquad (1)$$

where $\eta = \Delta^2\psi + f$. Here η is the absolute vorticity, ψ a stream function, f the Coriolis parameter and J the Jacobian operator. Since equation (1) simply states that the absolute vorticity is conserved following the fluid motion, an attractive alternative procedure can be based on following the motion of fluid elements in a Lagrangian manner. A technique for carrying out the integration in strict Lagrangian coordinates is presented by WIIN-NIELSEN (1959), but the rapid distortion of an initially square grid embedded in the flow limits the period over which the purely Lagrangian technique can be employed to 12 hours.

The technique described in the present paper traces the motion of fluid elements with respect to a fixed grid, attributing to each an appropriate value of absolute vorticity. At convenient intervals the wind field is reconstructed from the distribution of vorticity represented by the moving fluid elements and this wind field is employed to compute the further displacement of the fluid elements. The technique has the advantages that it closely parallels the physical interpretation of equation (1), and that it cannot artificially introduce vorticity not present in the original field (nor artificially remove it). Computational instability of the type associated with the Courant-Friedrichs-Lewy criterion does not arise and relatively long time steps may be employed.

2. The integration procedure

The steps taken in the course of the semi-Lagrangian integration of the vorticity advection equation may be summarised as follows:

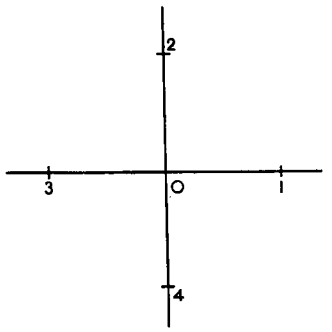

FIG. 1. Layout of points for computing vorticity.

(i) Form a list of fluid elements and their absolute vorticity, η, calculated from the initial stream function, ψ.
(ii) Calculate the advecting field, $\mathbf{V}$, from ψ.
(iii) Interpolate $\mathbf{V}$ to the positions of the fluid elements.
(iv) Calculate the displacements of the fluid elements over one time step.
(v) Delete from the list of fluid elements those leaving the area of the computation grid, and add to the list additional elements to represent the vorticity of air entering the area.
(vi) Form the field of relative vorticity, ζ $(=\nabla^2\psi)$, from the absolute vorticity of the fluid elements, η $(=\zeta+f)$.
(vii) Calculate the stream function, ψ, from the vorticity field, ζ.
(viii) Repeat from step (ii).

The following paragraphs give some more details of each step as carried out in the experiments reported here. The following notation is used.

Δ^2 is the simple finite difference approximation to the operator Δ^2. Thus $\Delta^2\psi = \{\psi_1+\psi_2+\psi_3+\psi_4-4\psi_0\}/h^2$ where h is the grid-length and ψ_0, ψ_1 etc. are the values of the stream function, ψ, at an array of point arranged as in Fig. 1.

η_r is the finite difference approximation to the vorticity of the rth fluid element at its initial position. T is the time-step.

Step (i). The initial list contained one entry for each point of the basic grid, excluding boundary points. With each fluid element was associated its initial absolute vorticity calculated from

$$\eta_r = \{\Delta^2\psi\}_{t=0} + f. \tag{2}$$

Steps (ii) and (iii). Following FJÖRTOFT (1955) and WINN-NIELSEN (1959) advection was carried out using winds derived from a smoothed stream function, ψ', where (in the notation of Fig. 1)

$$\psi'_0 = \tfrac{1}{4}(\psi_1+\psi_2+\psi_3+\psi_4). \tag{3}$$

Advecting velocities at grid-points were evaluated by simple two-point finite differences and linear interpolation used to the positions of the fluid elements.

Step (iv). At each time step except the first, the co-ordinates of each fluid element for use at the next time step were calculated from the centred difference relations

$$\left.\begin{aligned} X'_{t+1} &= X_{t-1} + 2u'_t T, \\ Y'_{t+1} &= Y_{t-1} + 2v'_t T, \end{aligned}\right\} \tag{4}$$

where x' and y' are preliminary co-ordinates for use at the next step. The values of x'_t and y'_y were subsequently corrected when u'_t had been calculated to give improved values.

$$\left.\begin{aligned} X_t &= X_{t-1} + \tfrac{1}{2}(u'_t + u'_{t-1})T, \\ Y_t &= Y_{t-1} + \tfrac{1}{2}(v'_t + v'_{t-1})T. \end{aligned}\right\} \tag{5}$$

At the first time step uncentred differences were used in place of (4).

Step (v). All fluid elements with new co-ordinates outside the boundary of the grid were deleted from the list before computation proceeded.

The results of the barotropic forecasts were found to be sensitive to the procedure adopted for introducing new fluid elements at inflow boundaries and several variants were tried. The procedure found most successful was as follows. The inflow velocity, v_n, normal to the boundary was computed at the first interior row of points from the stream function at the initial stage. A new fluid element was introduced at this point at the Nth time step if $v_n NT/h$ had increased beyond a new integer since the $(N-1)$th time step (thus a new fluid element was introduced every time an element moving inward with velocity, v_n, would have crossed a grid-line). The vorticity attributed to the new element was the initial vorticity at the point at which it was introduced. If $v_n NT/h$ increased past two or more integers in one time step, two or more new fluid elements were introduced, the addi-

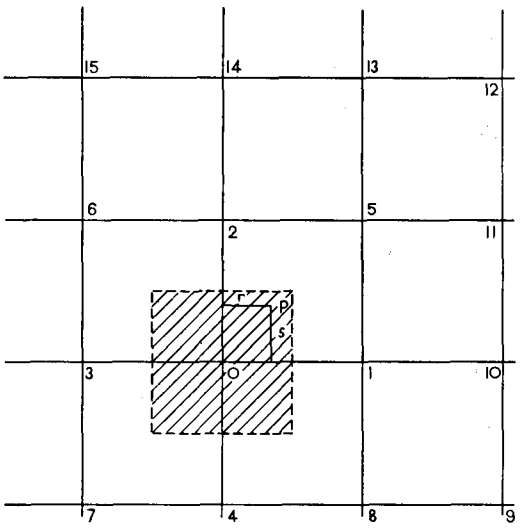

FIG. 2. Layout of points used in interpolation procedure.

tional elements being appropriately displaced into the computation area along the wind vector.

Step (vi). In order to form the field of vorticity at grid-points a weighted average of the vorticity of all fluid elements in a square of two grid-lengths side was used. It was obtained in the following manner:

(*a*) For each fluid element, for example at P in Fig. 2, the absolute vorticity, η, is allocated to the corner points 0, 1, 2 and 5 of the square in which it lies by multiplying by $(1-r)(1-S)$, $r(1-S)$, $(1-r)S$ and rS respectively. Subsequently the vorticity appropriate to each grid-point is determined from

$$\eta_P = \bar{f} + \sum_n [a_n(\eta - \bar{f})] / \sum_n a_n,$$

where the summation is over all fluid elements in the squares surrounding P and a_n represents the factor by which the vorticity of the fluid element has been multiplied. ($\bar{f}$ is the average value of the Corolius parameter.)

(*b*) If $n = 0$ a mean value, M, of η_P at surrounding grid points is substituted.

(*c*) The difference of vorticity totaled over grid points from that totaled over the fluid elements is shared between the grid points.

(*d*) The relative vorticity, ζ, is computed from

$$\zeta_P = \eta_P - f$$

Step (vii). The new field of the stream function, ψ_t, is calculated from the field of relative vorticity by means of the equation

$$\Delta^2 \psi_t = \zeta_P$$

This is solved by the usual iterative Liebmann process.

3. Experiments with the semi-Lagrangian technique on analytical fields

Some experiments have been conducted in which both the semi-Lagrangian technique and the more usual Eulerian scheme of integration have been applied to a stream function represented by the analytical expression

$$\psi = 2 - \frac{1}{1 + (x^2 + y^2)a^{-2}} - \frac{y}{b}$$

which represents a vortex embedded in a uniform current.

The true solution is known and represents a simple translation of the vortex along the x-axis.

For values of $a = 4$ or more corresponding to a vortex extending over some 8 grid-lengths the Eulerian method underestimated the motion of vortex by some 10 per cent as expected from the theoretically known truncation error when simple finite differences are used (MIYAKODA's (1962) 3–3–3 scheme). The semi-Lagrangian scheme was not subject to this effect and consequently had smaller errors. The under estimate of the vortex motion was, however, removed if a five-point formula was used to estimate derivatives in the advection Jacobian $J(\psi, \eta)$ (Miyakoda's 3–5–3 scheme) and the Eulerian scheme then gave somewhat better results than the semi-Lagrangian scheme.

However, when computations were carried out with smaller values of a (vortices extending over less than 8 grid-lengths) the semi-Lagrangian scheme gave significantly better results than the Eulerian scheme whichever finite difference scheme was employed. This is illustrated in Fig. 3 by calculations with $a = 1$ representing a vortex extending over little more than two grid lengths. Noteworthy is the tendency of the Eulerian schemes to increase the transverse wind behind the trough line and consequently to displace the vortex to the right of its track. It can be explained as an effect of the slower

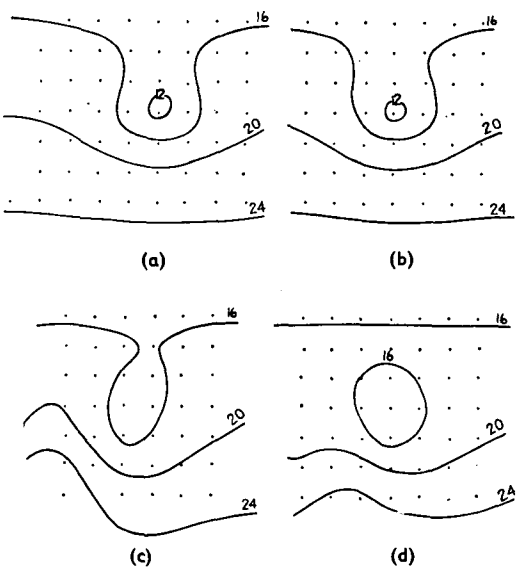

Fig. 3*a*. Correct stream function (or initial field displaced by 4 grid-lengths). *b*, Computed stream function by semi-Lagrangian procedure. *c*, Computed stream function by Eulerian (3–3–3) scheme. *d*, Computed stream function by Eulerian (3–5–3) scheme.

displacement of the short wavelength feature which define the trough line than of the longer wavelength components defining the outer part of the profile; a differential effect of truncation error.

4. Barotropic predictions at 500 mb with the semi-Lagrangian scheme

In order to test the suitability of the semi-Lagrangian scheme for use in preparing numerical forecasts, the technique was applied to a stream function derived from the 500 mb chart on ten occasions. The stream function was derived by solving the "balance equation" by the method of MIYAKODA (1960). At the conclusion of the 24-hour forecasts the balance equation was resolved again as a Poisson equation for the geopotential, h. Time steps of 6 hours were used on a 20×24 grid as used by KNIGHTING, CORBY & ROWNTREE (1962). For comparison, forecasts were also made by the Eulerian (3–3–3) scheme based on the same stream function and using 1-hour time steps. Statistics of the results are given in Table 1 for an interior area of 16×12 points as illustrated by KNIGHTING *et al.* (1962).

TABLE 1. *Verification statistics for 24-hr 500 mb barotropic forecasts prepared using a semi-Lagrangian method and a conventional finite difference method.*

	Semi-Lagrangian			Finite-difference		
Date	(*a*)	(*b*)	(*c*)	(*a*)	(*b*)	(*c*)
12.1.59	68	25	0.42	93	30	0.09
16.1.59	58	19	0.80	106	25	0.66
5.2.59	54	24	0.82	56	25	0.80
10.2.59	119	36	0.43	85	34	0.48
16.2.59	132	30	0.79	72	20	0.92
5.3.59	68	21	0.87	73	27	0.76
20.7.59	43	13	0.88	30	13	0.87
27.7.59	51	16	0.56	52	17	0.60
10.9.59	57	21	0.75	52	18	0.80
27.10.59	86	21	0.89	73	24	0.86
Mean	74	22.6	0.72	69	22.9	0.68

[a] r.m.s. error in predicted 500 mb height (metres).
[b] r.m.s. vector wind error (kts).
[c] Correlation coefficient between observed and predicted 500 mb height changes.

Overall there is little to choose between the verification statistics of the two schemes, but there are some interesting differences between the individual charts produced by the two methods. Such differences may arise from (*a*) the differences in the boundary conditions used in the two schemes and (*b*) from differences in the approximation to the solution of equation (1). The two effects can be recognised separately in the results.

The Eulerian scheme which was used held the stream function, ψ, constant throughout the integration at two rows of grid-points at the boundary. Near the inflow boundary it appeared to be largely fortuituous whether this led to a solution closer to the actual developments than the assumption of the semi-Lagrangian scheme which maintained ψ constant at a single row of points and continued the initial vorticity advection. However, on the whole the former procedure appeared less liable to extreme errors.

CHARNEY, FJÖRTOFT & NEUMANN (1950) showed that sufficient boundary conditions for solution of the barotropic vorticity equation are provided by specifying the stream function ψ at all points of the boundary and the vorticity η only at points of inflow. The boundary conditions employed with the Eulerian method

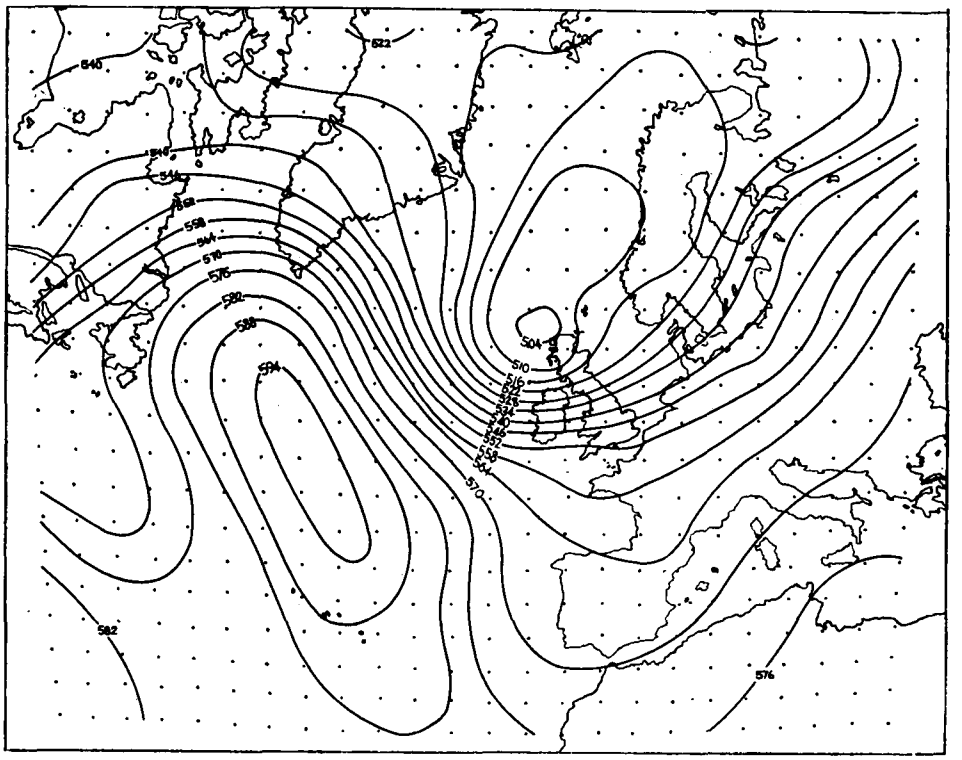

Fig. 4*a*. 500 mb contours 0000 GMT 27th October 1959 (dm).

which provide two conditions along all sections of the boundary, therefore probably over-specify the problem. An effect of this may be found in the considerable irregularities in the Eulerian solutions in areas adjacent to the outflow boundary. Although such irregularities appeared in several of the Eulerian solutions examined during the present study, they were absent from the corresponding semi-Lagrangian solutions.

As indicated in section 3 it might have been expected that in the synoptic examples studied the synoptic features, lows, troughs etc., would have been given greater displacements in the semi-Lagrangian integrations than by the Eulerian scheme. This effect was not, however, very noticeable in the results. Nevertheless, the positions of synoptic features did appear to be predicted somewhat better by the semi-Lagrangian method; the predicted position was classed as better in respect of 11 features, as good for 5 features and worse for 4 when a comparison was made with the Eulerian scheme.

Particularly interesting is the difference between the integrations based on the situation at 0000 GMT on 27th October 1959. This is illustrated in Figs. 4*a–d*. The movement of a low centre was predicted as SSE-wards by the Eulerian method (with simple finite differences), but the actual movement was ESE-ward and this was correctly given by the semi-Lagrangian method. There were no important differences between the two calculations over other areas of the chart and the differences in the result are believed to arise from the truncation error in the finite differences used in the Eulerian scheme. The error is similar to that illustrated in Fig. 3 and discussed in section 3.

5. Discussion

The semi-Lagrangian technique is shown to provide a practical method of integrating the barotropic vorticity–advection equation and may prove of use as a means of monitoring the truncation errors of the Eulerian schemes more

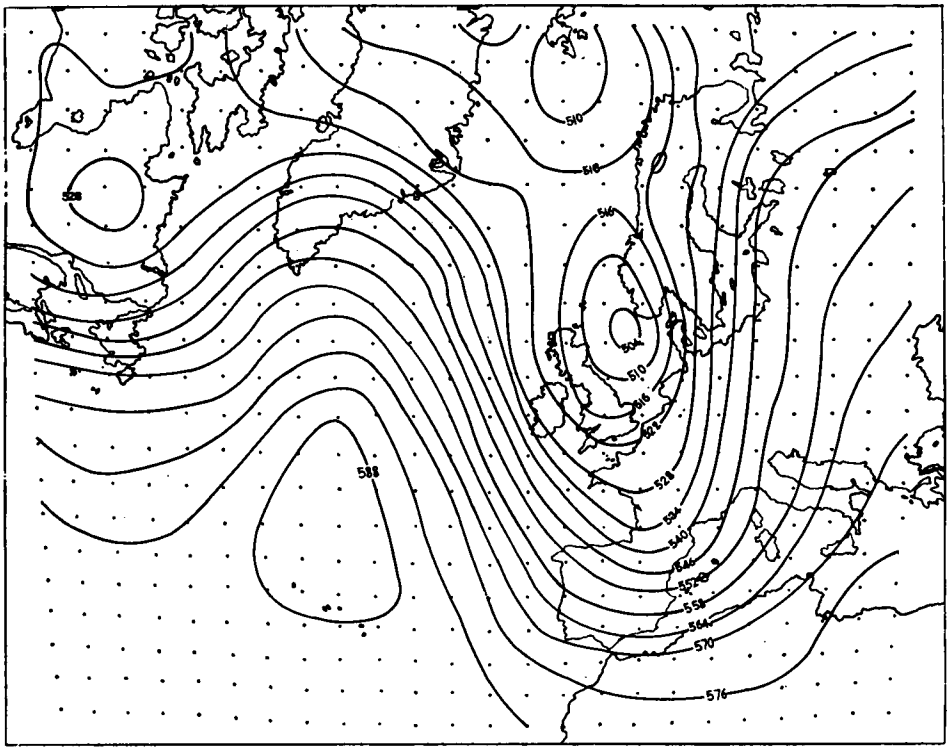

Fig. 4b. 500 mb contours 0000 GMT 28th October 1959 (dm).

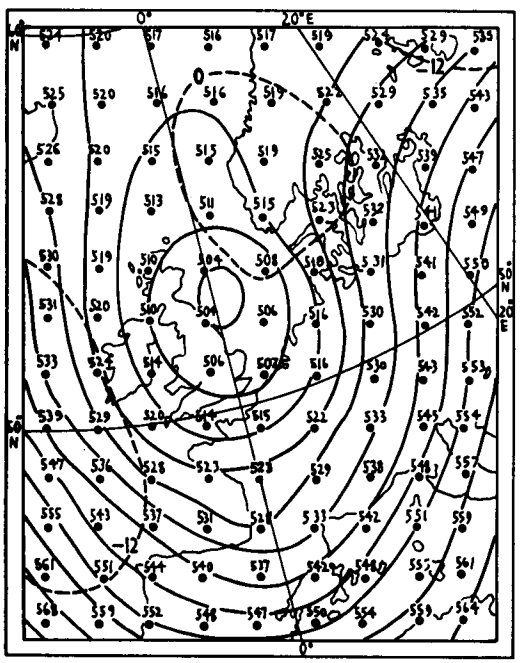

Fig. 4c. 500 mb contours computed by semi-Lagrangian method for 0000 GMT 28th October 1959 and distribution of error (dm).

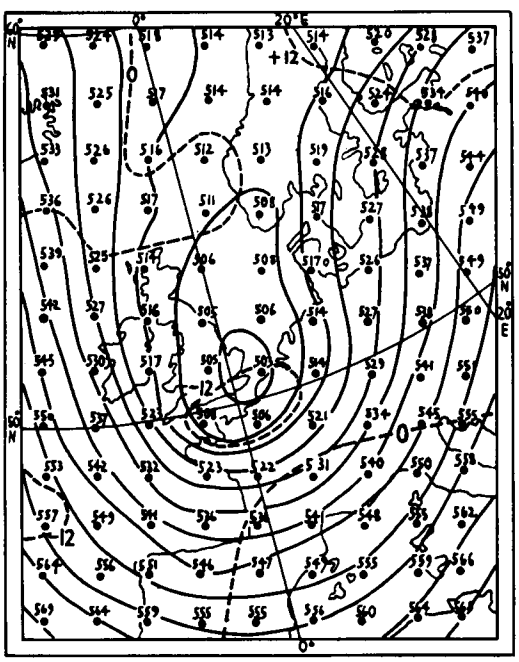

Fig. 4d. 500 mb contours computed by Eulerian (3–3–3) method for 0000 GMT 28th October 1959 and distribution of error (dm).

usually employed in numerical weather prediction.

The semi-Lagrangian technique permits time steps of 6 hours to be used without encountering computational instability and the method also creates less distortion than the Eulerian method when the scale of the features of the flow pattern falls to a few grid-lengths. The method may therefore have practical value, if limitations on computing resources necessitate the use of relatively coarse grids and long time steps.

Acknowledgements

This paper is published with the permission of the Director General of the Meteorological Office.

I also wish to acknowledge the valuable assistance of Miss J. Portnall in programming and carrying out the computations on the electronic computer, Meteor.

REFERENCES

CHARNEY, J. G., FJÖRTOFT, R., and VON NEUMANN, J., 1950, Numerical integration of the barotropic vorticity equation. *Tellus*, **2**, No. 4, pp. 237–254.

FJÖRTOFT, R., 1952, On a numerical method of integrating the barotropic vorticity equation. *Tellus*, **4**, pp. 179–194.

GATES, W. L., 1959, On the truncation error, stability and convergence of difference solutions of the barotropic vorticity equation. *J. of Meteorol.*, **16**, pp. 556–568.

GATES, W. L., and RIEGEL, C. A., 1962, A study of numerical errors in the integration of barotropic flow on a spherical grid. *J. of Geophys. Res.*, **67**, pp. 773–784.

KNIGHTING, E., CORBY, G. A., and ROWNTREE, P. R., 1962, An experiment in operational numerical weather prediction. London, Meteorological Office, Scientific Paper No. **16**, 28 p.

MIYAKODA, K., 1960, Numerical solution of the balance equation, Japanese Meteorological Agency, Technical Report No. **3**, pp. 15–34.

MIYAKODA, K., 1962, A trial of 500 hour barotropic forecast. *Proc. Int. Symp. Numerical Weather Prediction in Tokyo*, pp. 221–240.

WINN-NIELSEN, A., 1959, On the application of trajectory methods in numerical forecasting. *Tellus*, **11**, pp. 180–196.